Plant Syst Evol (2014) 300:1877–1893
DOI 10.1007/s00606-014-1014-z

ORIGINAL ARTICLE

Fine structure of *Quercus* pollen from the Holocene sediments of the Sea of Japan

Maria V. Tekleva · Natalia N. Naryshkina · Tatiana A. Evstigneeva

Received: 23 November 2013 / Accepted: 8 February 2014 / Published online: 16 May 2014

Abstract Holocene dispersed pollen from two cores from the shelf zone of the Korean Bay and from the deep water zone of the south of the Sea of Japan were studied by means of light and electron (scanning and transmission) microscopy. Three sculpture types were observed: rod-like, rugulate-granulate and (micro)verrucate. Ten conventional groups were separated according to the sporoderm morphology and ultrastructure. Possible specific attribution was suggested based on the comparison with published data on modern and fossil oak pollen. The perspective of further application of electron microscopy for this taxon is discussed.

Keywords *Quercus* · Pollen · Sculpture · Ultrastructure · Systematics

Introduction

Oak pollen grains are an important component of Cenozoic palynological assemblages and are often both well represented and useful for interpretation of the paleovegetation and paleoclimate. Due to the numerous species of diverse ecological preferences the genus *Quercus* has been studied in the hope of finding additional characters for the precise determination of their pollen, which so far are mostly recognized at the generic level. First, these were studies on the level of light microscopy (LM), which showed that the aperture condition, sculpture, and pollen size are most important (see review in Naryshkina 2013). Further, it became clear that for this purpose and due to the small pollen size higher magnifications of electron microscopes are needed to obtain more accurate information.

Data on modern oak pollen are exceptionally important for a comparative analysis and reliable attribution of the dispersed pollen grains to particular oak species. Such works confirmed a perspective on the use of scanning electron microscopy (SEM) for this genus (see a detailed review in Liu et al. 2007). Various studies appeared: reports on pollen morphology of different geographic regions (e.g., Solomon 1983a, b; Medus and Gonzalez-Flores 1984; Makino et al. 2009; Van Benthem et al. 1984; Wang and Pu 2004), pollen ontogeny (Rowley and Gabaraeva 2004), pollen degradation (Kedves et al. 2002; Rowley and Skvarla 1994; Skvarla et al. 1996), and an analysis of the significance of pollen characteristics in *Quercus* (Liu et al. 2007; Denk and Grimm 2009). This served as a base for the infrageneric identifications of oak pollen of some deciduous and evergreen species, systematics, and possible relationships between species that possess different morphological types (Yamazaki and Takeoka 1959; Nakagawa et al. 1996; Ferguson et al. 1998; Liu et al. 2007; Denk et al. 2010, 2012; Naryshkina and Evstigneeva 2009; Evstigneeva and Naryshkina 2012). Several general morphological types of *Quercus* pollen were outlined with consideration of the deciduous or evergreen habit of the plants; others are still necessary to be checked or to be distinguished. More data should be accumulated for the accurate recognition of dispersed oak pollen at the level of species.

M. V. Tekleva (✉)
Borissiak Paleontological Institute, Russian Academy of Sciences, Profsojuznaya str., 123, Moscow, Russia
e-mail: tekleva@mail.ru

N. N. Naryshkina · T. A. Evstigneeva
Institute of Biology and Soil Science, Far Eastern Branch, Russian Academy of Sciences, Prospect Stoletiya Vladivostoka 159, Vladivostok, Russia

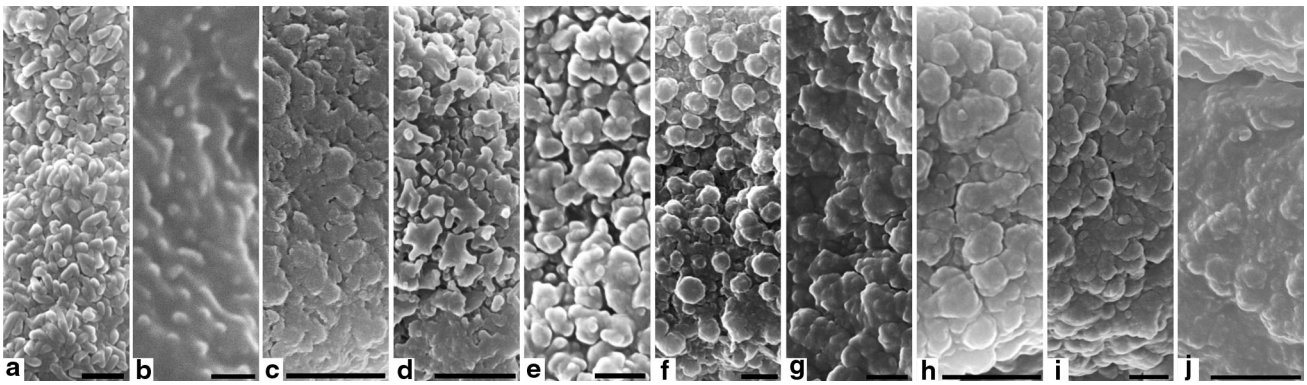

Fig. 1 Exine sculpturing in SEM. **a** Group 1; **b** Group 2; **c** Group 3; **d** Group 4; **e** Group 5; **f** Group 6; **g** Group 7; **h** Group 8; **i** Group 9; **j** Group 10. *Scale bar* 0.5 μm in **b**; 1 μm in **a**, **e**–**g**, **i** 2 μm in **d**, **h**; 2.5 μm in **c**, **j**

Here, we contribute by studying dispersed pollen grains from the Holocene deposits of the Sea of Japan not only by means of LM and SEM, but also by transmission electron microscopy (TEM). This is the first attempt to our knowledge of studying the sporoderm ultrastructure of fossil dispersed oak pollen grains.

Material and methods

The material comes from marine bottom sediments from the south of the Sea of Japan. Dispersed *Quercus* pollen from eight palynological samples of two cores (2747 and J3) were studied. The core 2747 is from the shelf zone of the Korean Bay. Six samples belonging to two palynological assemblages (II and III) from the following depths were studied: 40–45, 80–85, 130–135, 170–178, 205–213, and 265–275 cm. Palynological assemblage II (core 2747, 275–135 cm) corresponds to the Preboreal and Boreal phases of the Holocene, and palynological assemblage III (core 2747, 135–10 cm) to the Atlantic phase. The core J3 is from the deep water zone of the south of the Sea of Japan. Two samples belonging to two palynological assemblages (II and V) from the following depths were studied: 80–82 and 500–502 cm. Palynological assemblage II (core J3, 510–430 cm) corresponds to the Preboreal and Boreal phases of the Holocene, and palynological assemblage V (core J3, 93–0 cm) corresponds to the Subatlantic phase. Detailed information on the assemblages can be found in Naryshkina and Evstigneeva (2009) and Evstigneeva and Naryshkina (2012).

Individual pollen grains were studied subsequently with light microscopy (LM), scanning electron microscopy (SEM) and, for a number of specimens, transmission electron microscopy (TEM) (20–25 grains from each sample). Pollen grains were picked up from the residue and photographed in LM (Zeiss Axioplan-2), then removed from the slide and after washing in ethanol mounted on SEM stubs on small pieces of film. The pieces were affixed to the stub using nail polish with its upward emulsive covering. The stubs were sputter coated with platinum–palladium or gold. Pollen grains were observed and photographed under a Camscan SEM, JSM, Zeiss EVO 40 and Tescan. For TEM some pollen grains were removed from the stubs and some of them were fixed with 1 % OsO_4 and then embedded in epoxy resin according to Meyer-Melikyan et al. (2004). Others were directly embedded in epoxy resin. Pollen grains were sectioned with an LKB Ultratome V, ultramicrotome LKB-3 and Leica UC6. The ultrathin sections were stained with lead citrate and uranyl acetate for some pollen grains and examined under Jeol 100 B and Jeol 1011 TEMs. Some sections were studied unstained. The terminology used is after Hesse et al. (2009).

Results

Pollen grains are medium-sized, prolate, tricolpate or tricolporate. They are mostly compressed along the polar axis (i.e., only equatorial view is available), though some are compressed along the equatorial diameter. The exine sculpture in LM is scabrate to granulate and in SEM microverrucate to verrucate, rarely rugulate–granulate or of rod-like elements with perforations which sometimes are difficult to distinguish. In TEM the sporoderm consists of the tectum of different thickness, columellar infratectum and rather thin, discontinuous foot layer, and thin endexine with discrete thickenings ("drops of thickenings"). Toward the aperture regions the ectexine reduces in thickness, usually the columellae disappear first, and then the tectum and foot layer, with the latter sharply becoming thinner.

Table 1 Measurements of the studied oak pollen

Group	Size (LM), ExP, μm	Size (SEM), ExP, μm	Sculpture (SEM)	Extexine thickness, μm	Tectum thickness, μm	Columella height, μm	Columella width, μm	Foot layer thickness, μm
1	18.3 × 24.5	15.5 × 25.0	Rod-like	1.0 (0.88–1.08)	0.63 (0.48–0.67)	0.1 (0.6–0.11)	0.17 (0.13–0.27)	0.2 (0.17–0.28)
2	18.4 × 26.5	16.8 × 24.4	Rugulate–granulate	0.8 (0.65–0.95)	0.35 (0.28–0.5)	0.2 (0.15–0.24)	0.17 (0.12–0.22)	0.03 to 0.29
3	15.5–26.0 × 24.6–32.6	18.2–25.0 × 25.2–32.7	Flattened (micro)verrucate, perforated	0.42–1.08	0.13–0.55	0.15–0.31	0.09–0.42	0.03–0.33
4	20.0–30.3 × 26.3–39.4	18.9–27.9 × 26.0–36.4	(Micro)verrucate, verrucae flattened, stellate-like	0.5–1.2	0.16–0.75	0.13–0.36	0.14–0.40	0.13–0.39
5	16.4–29.2 × 23.1–39.2	12.9–26.7 × 23.7–37.0	(Micro)verrucate, verrucae flattened, rounded-angular	0.44–1.75	0.1–1.25	0.1–0.52	0.07–0.49	0.04–0.42
6	19.5–29.7 × 30.0–37.6	18.2–28.5 × 28–36.2	(Micro)verrucate, verrucae not flattened, standing alone	0.42–1.11	0.1–0.65	0.11–0.3	0.07–0.42	0.04–0.25
7	24.6–33.5 × 35.7–45.6	21.7–30.0 × 31.1–43.0	Microverrucate, verrucae flattened and distinctly granulate, forming islands	0.45–0.75	0.1–0.34	0.11–0.25	0.17–0.34	0.05–0.17
8	15.1–24.8 × 28.8–36.0	13.7–25.5 × 25.1–41.5	(Micro)verrucate, verrucae often forming islands	0.68–0.94	0.13–0.53	0.13–0.27	0.22–0.31	0.04–0.15
9	16.1–30.0 × 23.1–37.3	11.4–27.7 × 19.4–34.6	Microverrucate, verrucae of different sizes, flattened or rounded, often closeby	0.37–1.32 (mostly 0.45–0.9)	0.1–0.71 (mostly up to 0.55)	0.09–0.42	0.08–0.42	0.02–0.36 (mostly up to 0.2)
10	18.9–25.3 × 27.9–37.5	17.7–26.8 × 26.8–35.4	Microverrucate, verrucae of different sizes, mostly flattened, scattered	0.38–1.0	0.1.52	0.08–0.13	0.08–0.44	0.02–0.15

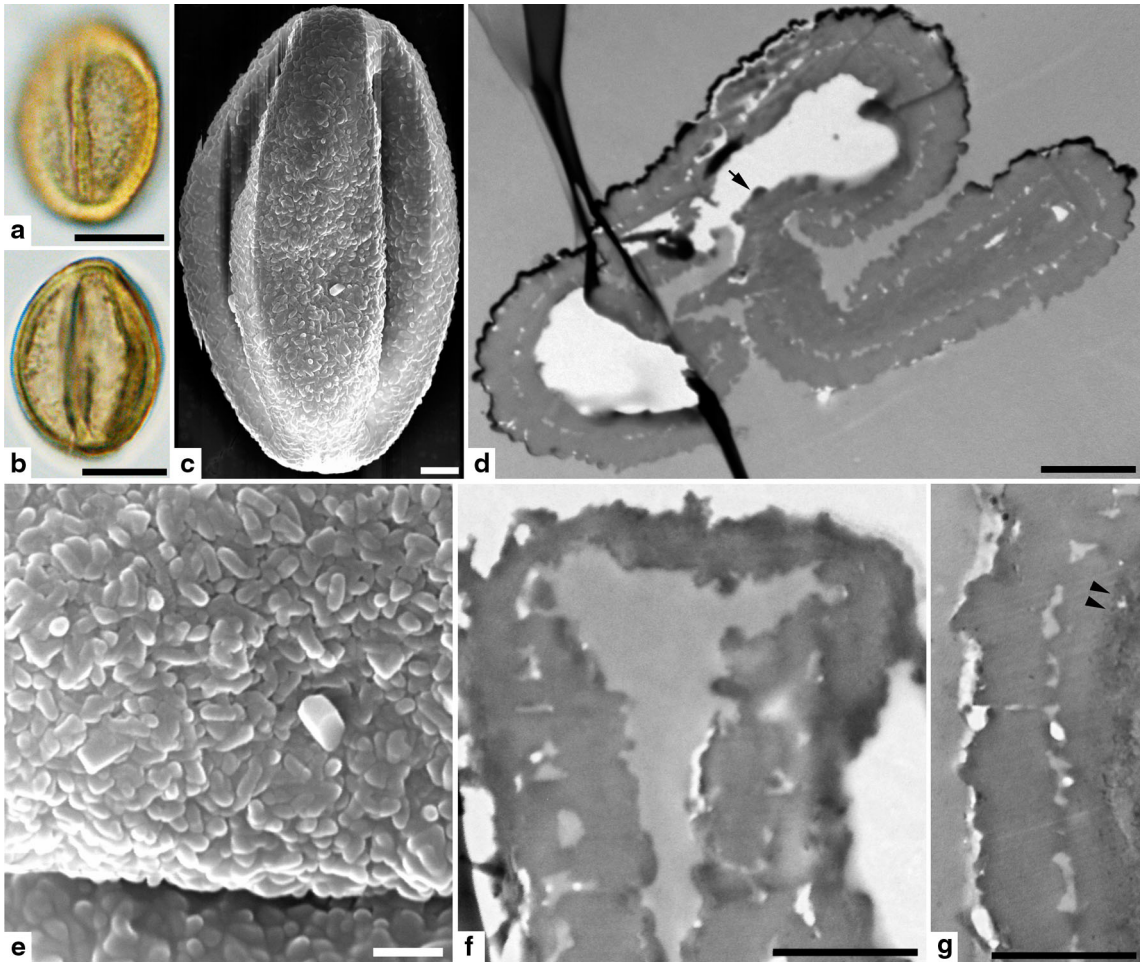

Fig. 2 Pollen morphology and ultrastructure of Group 1 (**a**–**g**). **a**, **b** LM, equatorial view, two different foci; **c** SEM, equatorial view; **d** section through the whole pollen; *arrow* indicates aperture region; **e** SEM, exine sculpturing; **f** TEM, aperture region; **g** TEM nonaperture regions, *arrowheads* show border between ect- and endexine. *Scale bar* 1 μm for **e**–**g**; 2 μm for **c**, **d**; 10 μm for **a**, **b**

The endexine becomes thicker toward the aperture regions, though the layer is not always well preserved. The studied pollen grains have been separated into 10 groups mostly considering their sculpture pattern (Fig. 1a–j; Table 1).

Group 1: one pollen grain from core 2747: 80–85 cm (Fig. 2a–g)

The pollen grain is 18.3 × 24.5 μm as measured in LM, and 15.5 × 25.0 μm in SEM, prolate and tricolpate to tricolporoidate. The sculpture in SEM is formed of intercrossed rod-like elements which are oriented in different directions. Perforations are difficult to distinguish. In TEM the ectexine is about 1.0 (0.88–1.08) μm thick. The tectum is about 0.63 (0.48–0.67) μm thick with strongly undulate outer contour and canals about 0.03 μm in diameter through to the infratectum. The columellae are about 0.1 (0.6–0.11) μm high and 0.17 (0.13–0.27) μm wide, the foot layer is mostly continuous and about 0.2 (0.17–0.28) μm thick. There is a more electron-dense layer beneath the foot layer (probably the endexine) from 0.12 to 0.2 μm in thickness.

Group 2: one pollen grain from core J3: 80–82 cm (Fig. 3a–g)

The pollen grain is 18.4 × 26.5 μm as measured in LM, and 16.8 × 24.4 μm in SEM, prolate, tricolpate, or tricolporoidate. The sculpture in SEM is rugulate–microechinate, microechini up to 0.1 μm in diameter. Perforations are not apparent. In TEM the ectexine is about 0.8 (0.65–0.95) μm thick. The tectum is about 0.35 (0.28–0.5) μm thick with undulate outer contour corresponding to the sculpture pattern. Frequent canals of about 0.08–0.1 μm in diameter and holes up to 0.35 μm in diameter occur in the tectum. The columellae are about 0.2

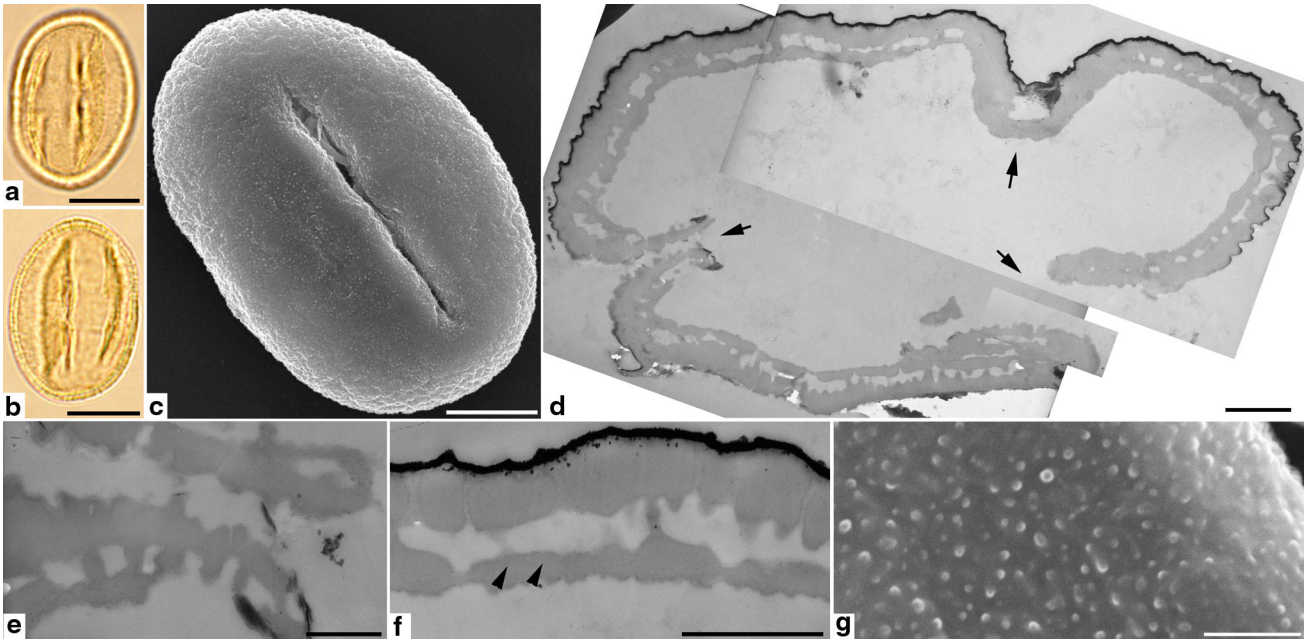

Fig. 3 Pollen morphology and ultrastructure of Group 2 (**a**–**g**). **a**, **b** LM, equatorial view, two different foci; **c** SEM, equatorial view; **d** TEM, section through the whole pollen; *arrow* indicates aperture region; **e** TEM, aperture region; **f** TEM, nonaperture region, *arrowheads* show border between ect- and endexine; **g** SEM, exine sculpturing. *Scale bar* 0.5 μm for **e**; 1 μm for **f**, **g**; 1.25 μm for **d**; 5 μm for **c**; 10 μm for **a**, **b**

(0.15–0.24) μm high and 0.17 (0.12–0.22) μm wide, and the foot layer is discontinuous and from 0.03 to 0.29 μm. The probable endexine is slightly less electron dense than the overlying exine and from 0.03 to 0.2 μm in thickness.

Group 3: pollen grains from core 2747: 80–85, 130–135, 170–178, 205–213 cm (Fig. 4a–g)

Pollen grains are 15.5–26.0 × 24.6–32.6 μm as measured in LM, and 18.2–25.0 × 25.2–32.7 μm in SEM, prolate and tricolpate to tricolporoidate. The sculpture in SEM is flattened verrucate or microverrucate, microrugulate, perforated, and fossulate. In TEM the ectexine thickness varies from 0.42 to 1.08 μm in the regions of (micro)verrucae or between them. Similarly, the tectum is from 0.13 to 0.55 μm thick with canals of different diameters and rises corresponding to (micro)verrucae. The columellae are about 0.15–0.31 μm high and 0.09–0.42 μm wide; the foot layer is discontinuous and from 0.03 to 0.33 μm thick. The probable endexine is slightly less electron dense and from 0.02 to 0.3 μm in thickness.

Group 4: pollen grains from core 2747: 40–45, 80–85, 130–135, 205–213 cm (Fig. 5a–g)

Pollen grains are 20.0–30.3 × 26.3–39.4 μm as measured in LM, and 18.9–27.9 × 26.0–36.4 μm in SEM, prolate, tricolpate. The sculpture in SEM is verrucate or microverrucate: sculptural elements are about or <1 μm in diameter, flattened, stellate-like with protruding rod-like elements in different sides, between (micro)verrucae there are tips of numerous solitary rod-like elements. Perforations are difficult to distinguish. In TEM the ectexine thickness varies from 0.5 to 1.2 μm in the regions of verrucae/microverrucae or between them. Similarly, the tectum is from 0.16 to 0.75 μm thick. Canals through the tectum to the infratectum are rare. The columellae are from 0.13 to 0.36 μm high and from 0.14 to 0.4 μm wide. The foot layer is of an uneven thickness, though it is only rarely discontinuous and mostly between 0.13 and 0.39 μm. The probable endexine is slightly less electron dense, from 0.08 to 0.34 μm in thickness, with sharp drops of the thickness, forming pud-like regions.

Group 5: pollen grains from core 2747: 40–45, 80–85, 130–135, 205–213, 265–275 cm, core J3: 500–502 cm (Fig. 6a–h)

Pollen grains are 16.4–29.2 × 23.1–39.2 μm as measured in LM, and 12.9–26.7 × 23.7–37.0 μm in SEM, prolate, tricolpate, or tricolporoidate. The sculpture in SEM is verrucate or microverrucate: sculptural elements are mostly <1 μm in diameter, flattened, rounded-angular; between (micro)verrucae there are tips of numerous solitary rod-like

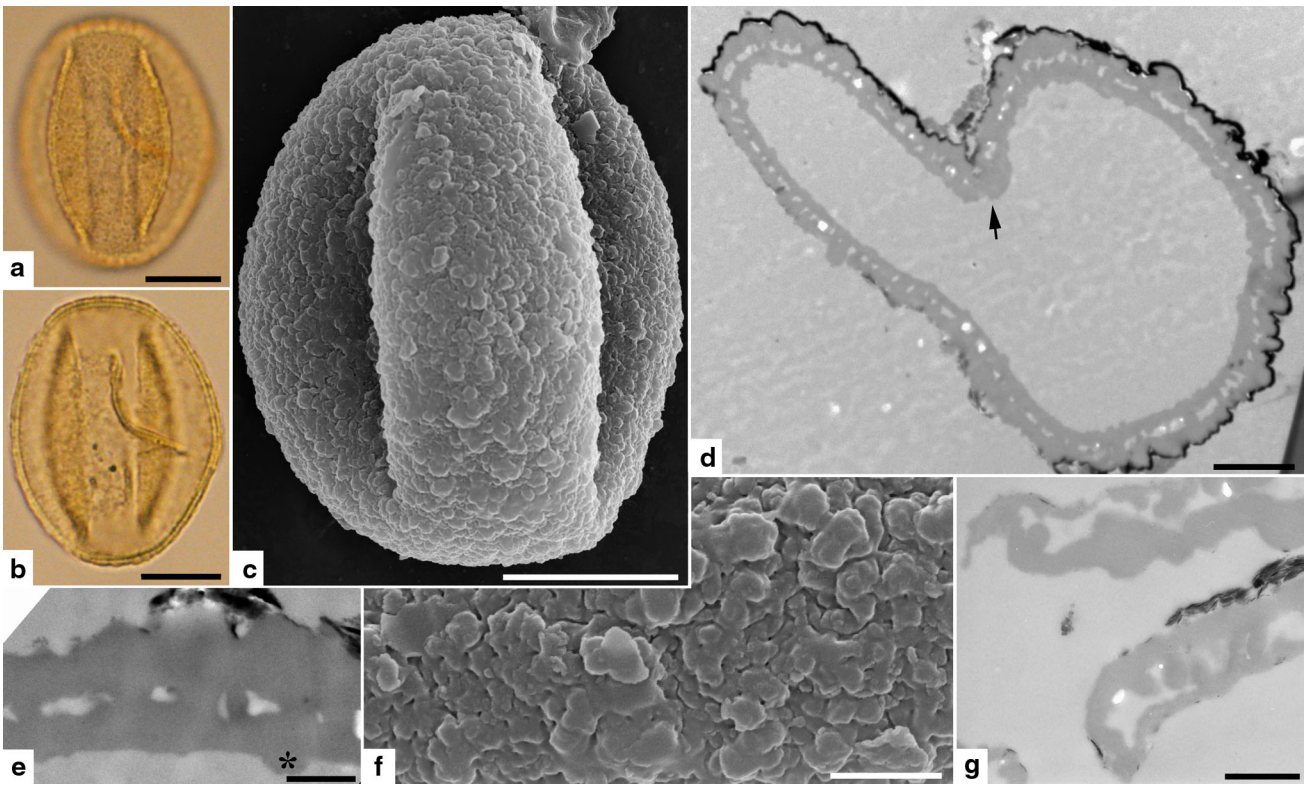

Fig. 4 Pollen morphology and ultrastructure of Group 3 (**a**–**g**). **a**, **b** LM, equatorial view, two different foci; **c** SEM, equatorial view; **d** TEM, section through the whole pollen; *arrow* indicates aperture region; **e** TEM, nonaperture region; *asterisk* shows endexine drop; **f** SEM, exine sculpturing; **g** TEM, aperture region. *Scale bar* 0.5 μm for **e**; 0.67 μm for **g**; 2 μm for **d**, **f**; 10 μm for **a**–**c**

elements. The (micro)verrucae are similar to those of Group 4, but are much more rounded and flattened. It seems that there is more sporopollenin material between rod-like elements, which form the (micro)verrucae in comparison to Group 4. Perforations are rare and not apparent. In TEM the ectexine thickness varies from 0.44 to 1.75 μm in the regions of microverrucae or between them. Similarly, the tectum is from 0.1 to 1.25 μm thick. The canals through to the infratectum are rare. The columellae are from 0.1 to 0.52 μm high and from 0.07 to 0.49 μm wide. The foot layer is of an uneven thickness, though it is not often discontinuous and mostly between 0.04 and 0.42 μm. The probable endexine is slightly less electron dense, from 0.03 to 0.52 μm in thickness, with sharp drops of the thickness, forming pud-like regions.

Group 6: pollen grains from core 2747: 40–45, 80–85 cm, core J3: 500–502 cm (Fig. 7a–j)

Pollen grains are 19.5–29.7 × 30.0–37.6 μm as measured in LM, and 18.2–28.5 × 28–36.2 μm in SEM, prolate and tricolpate to tricolporoidate. The sculpture in SEM is verrucate or microverrucate: sculptural elements are mostly <1 μm in diameter, most often about 0.5 μm, not flattened, of a regular rounded outlines, densely situated, mostly with each (micro)verruca standing alone and not merging with adjacent ones. On the surface of (micro)verrucae, poorly seen microechini can be distinguished (probably the former rod-like elements, covered with more sporopollenin masses). Between the (micro)verrucae the exine surface appears to be formed by rod-like elements, covered with sporopollenin masses. Perforations are not apparent. In TEM the ectexine thickness varies from 0.42 to 1.11 μm in the regions of (micro)verrucae or between them. Similarly, the tectum is from 0.1 to 0.65 μm thick. The canals through to the infratectum are extremely rare if they occur at all in some grains. The columellae are from 0.11 to 0.3 μm high and from 0.07 to 0.42 μm wide. The foot layer is of an uneven thickness, though it is not often discontinuous and mostly between 0.04 and 0.25 μm. The probable endexine is slightly less electron dense, from 0.02 to 0.33 μm in thickness, with sharp drops of the thickness, forming pud-like regions.

Group 7: pollen grains from core 2747: 40–45, 80–85, 170–178 cm, core J3: 80–82, 500–502 cm (Fig. 8a–i)

Pollen grains differ in LM from pollen of other groups; on the whole they are larger than in other groups, 24.6–33.5 × 35.7–45.6 μm as measured in LM, and

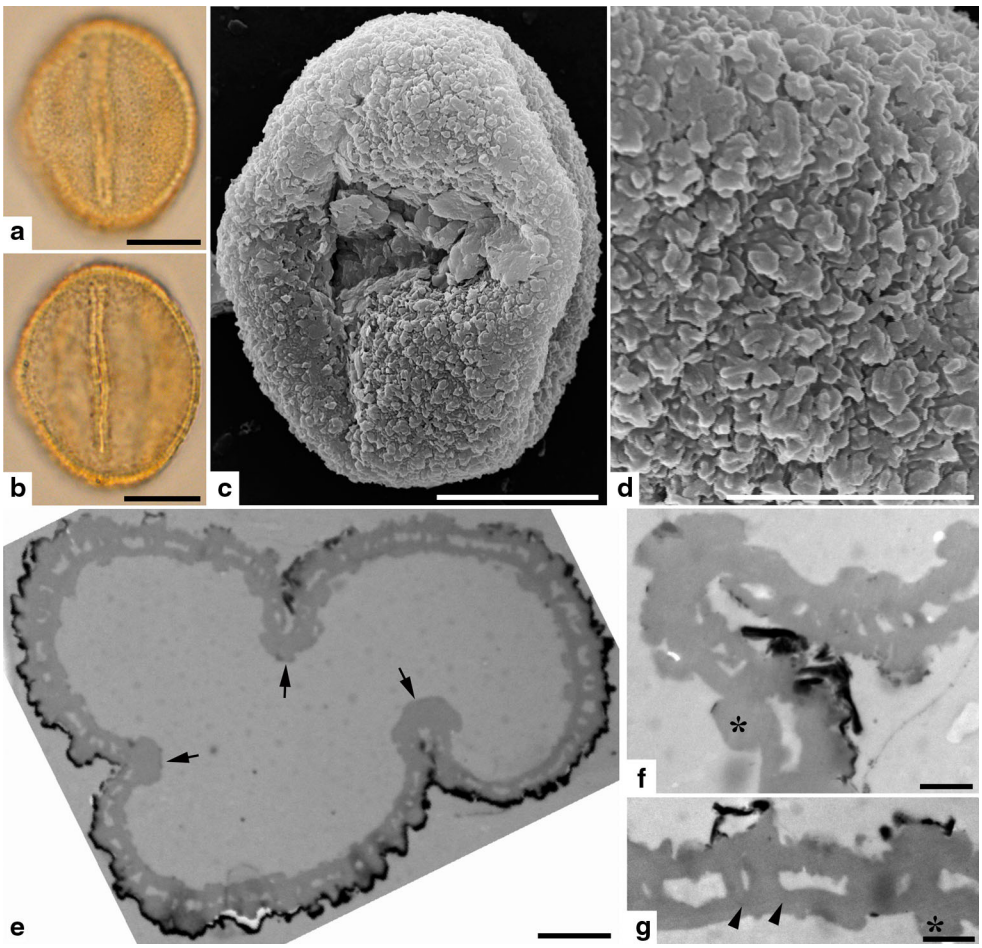

Fig. 5 Pollen morphology and ultrastructure of Group 4 (**a**–**g**). **a**, **b** LM, equatorial view, two different foci; **c** SEM, equatorial view; **d** SEM, exine sculpturing; **e** TEM, section through the whole pollen; **f** TEM, aperture region; **g** TEM, nonaperture region. *Arrowheads* show border between ect- and endexine; *asterisk* shows endexine drop; *arrow* indicates aperture region. *Scale bar* is 0.5 μm for **f**, **g**; 2 μm for **e**; 5 μm for **d**; 10 μm for **a**–**c**

21.7–30.0 × 31.1–43.0 μm in SEM, prolate and tricolpate. The sculpture in SEM is microverrucate: sculpture elements are of different sizes up to 1 μm and most of the larger elements are between 0.5 and 1 μm. The microverrucae are flattened and often connected with each other, forming islands. The surface of those is distinctly microechinate (probably these are tips of former rod-like elements covered with sporopollenin masses) as well as the surface between microverrucae. Perforations are rarely seen. In TEM the ectexine thickness varies from 0.45 to 0.75 μm in the regions of microverrucae or between them. Similarly, the tectum is from 0.1 to 0.34 μm thick. The canals through to the infratectum are occasionally seen. The columellae are from 0.11 to 0.25 μm high and from 0.17 to 0.34 μm wide. The foot layer is of an uneven thickness, though it is not often discontinuous and mostly between 0.05 and 0.17 μm. The probable endexine is slightly less electron dense, from 0.03 to 0.16 μm in thickness, with sharp drops of the thickness, forming pud-like regions.

Group 8: pollen grains from core 2747: 40–45, 80–85, 130–135 cm (Fig. 9a–f)

Pollen grains are 15.1–24.8 × 28.8–36.0 μm as measured in LM, and 13.7–25.5 × 25.1–41.5 μm in SEM, prolate and tricolpate to tricolporoidate. The sculpture in SEM is verrucate or microverrucate: sculptural elements are often grouped forming "islands" (aggregations). On the surface of (micro)verrucae microechini can be distinguished (probably the former rod-like elements, covered with additional sporopollenin). Perforations are not seen. In TEM the ectexine thickness varies from 0.68 to 0.94 μm in the regions of microverrucae or between them. Similarly, the tectum is from 0.13 to 0.53 μm thick. The canals through to the infratectum are occasionally seen. The

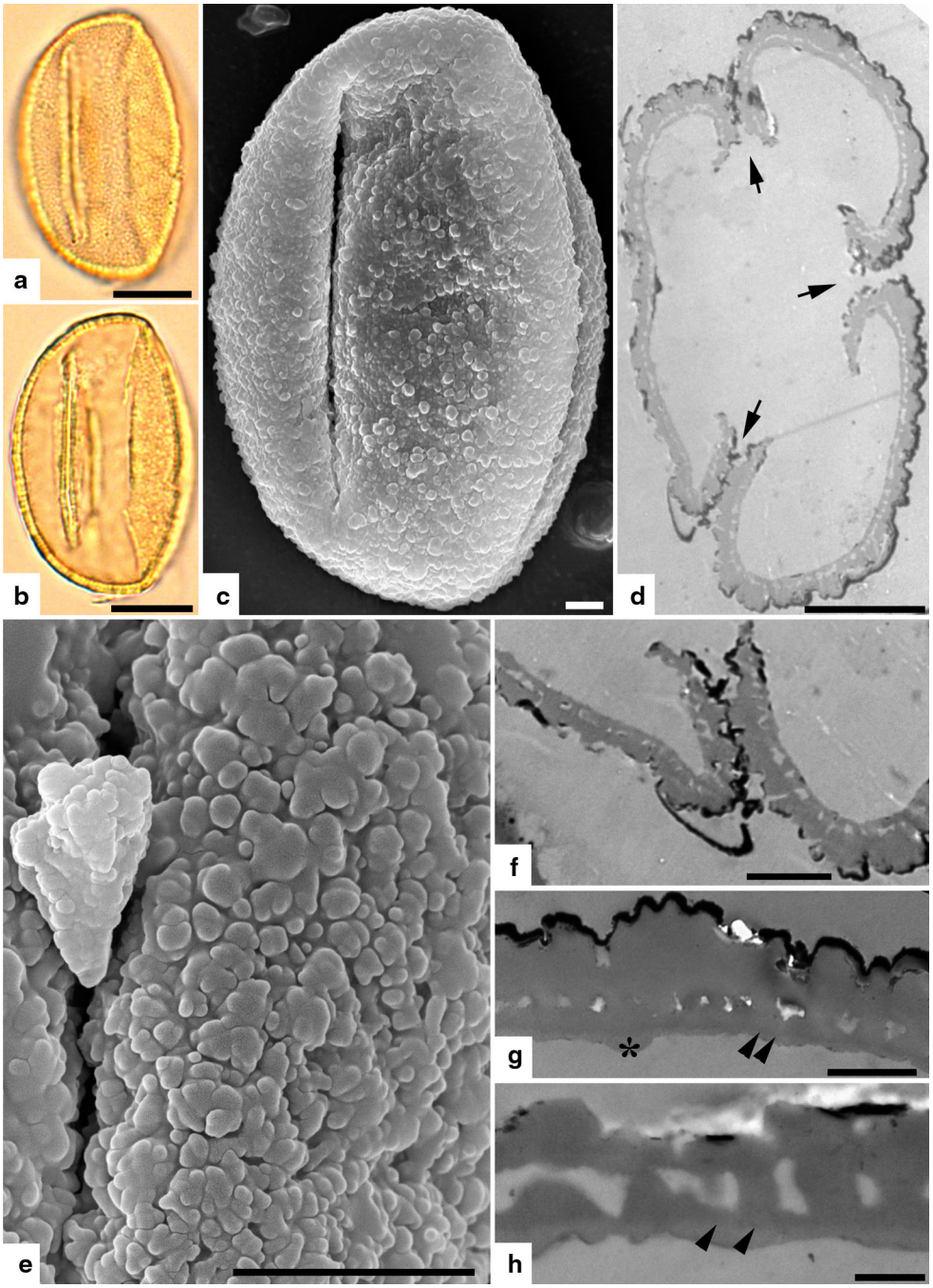

Fig. 6 Pollen morphology and ultrastructure of Group 5 (**a**–**h**). **a**, **b** LM, equatorial view, two different foci; **c** SEM, equatorial view; **d** TEM, section through the whole pollen; **e** SEM, exine sculpturing; **f** TEM, aperture region; **g**, **h** TEM, nonaperture region. *Arrowheads* show border between ect- and endexine; *asterisk* shows endexine drop; *arrow* indicates aperture region. *Scale bar* is 0.5 μm for **h**; 1 μm for **g**; 2 μm for **c**, **f**; 5 μm for **d**, **e**; 10 μm for **a**, **b**

columellae are from 0.13 to 0.27 μm high and from 0.22 to 0.31 μm wide. The foot layer is of an uneven thickness, though it is not often discontinuous and mostly between 0.04 and 0.15 μm. The probable endexine is slightly less electron dense, from 0.08 to 0.1 μm in thickness, with sharp drops of the thickness, forming pud-like regions.

Group 9: pollen grains from core 2747: 80–85, 130–135, 170–178, 205–213, 265–275 cm, core J3: 80–82 cm (Fig. 9g–n)

Pollen grains are 16.1–30.0 × 23.1–37.3 μm as measured in LM, and 11.4–27.7 × 19.4–34.6 μm in SEM, prolate

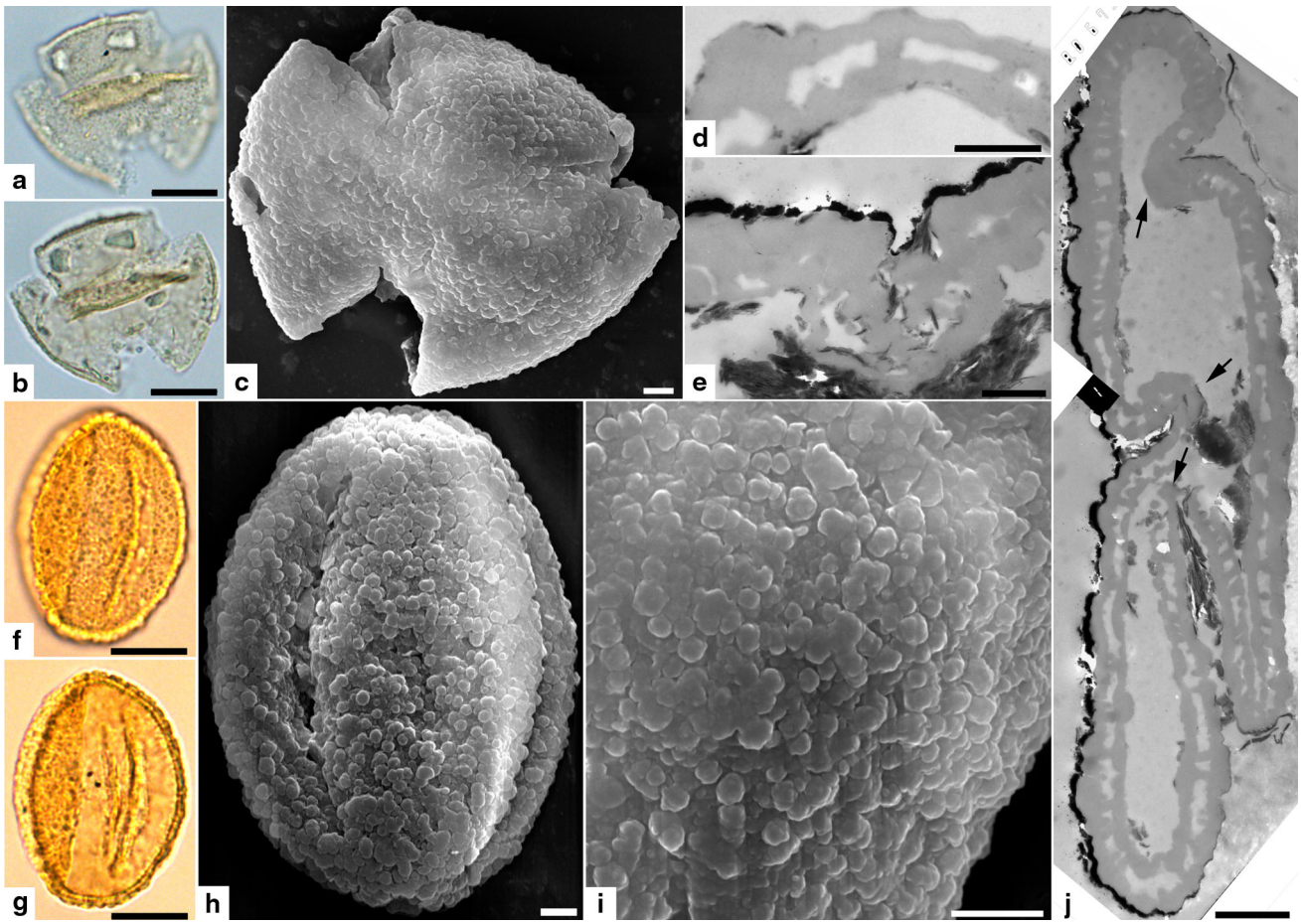

Fig. 7 Pollen morphology and ultrastructure of Group 6 (**a**–**j**). **a**, **b** LM, polar view, two different foci; **c** SEM, polar view; **d** TEM, nonaperture region; **e** TEM, aperture region; **f**, **g** LM, equatorial view, two different foci; **h** SEM, equatorial view; **i** SEM, exine sculpturing; **j** TEM, section through the whole pollen; *arrow* indicates aperture region. *Scale bar* is 0.5 μm for **d**; 0.67 μm for **e**; 1.25 μm for **j**; 2 μm for **c**, **h**, **i**; 10 μm for **a**, **b**, **f**, **g**

and tricolpate. The sculpture in SEM is microverrucate: sculptural elements varying in size, often flattened, mostly rounded in outline, and closely spaced. On the surface of the microverrucae sometimes poorly seen microechini can be distinguished (probably the former rod-like elements, covered with more sporopollenin masses). Perforations are not seen. In TEM the ectexine thickness varies from 0.37 to 1.32 (mostly 0.45–0.9) μm in the regions of microverrucae or between them. Similarly, the tectum is from 0.1 to 0.71 (mostly up to 0.55) μm thick. Canals through to the infratectum are occasionally seen. The columellae are from 0.09 to 0.42 μm high and from 0.08 to 0.42 μm wide. The foot layer is of an uneven thickness, though it is not often discontinuous and mostly between 0.02 and 0.36 (mostly up to 0.2) μm. The probable endexine is slightly less electron dense, from 0.02 to 0.45 μm in thickness, with sharp drops of the thickness, forming pud-like regions.

Group 10: pollen grains from core 2747: 40–45, 130–135, 170–178, 205–213, 265–275 cm (Fig. 10a–h)

Pollen grains are 18.9–25.3 × 27.9–37.5 μm as measured in LM, and 17.7–26.8 × 26.8–35.4 μm in SEM, prolate and tricolpate. The sculpture in SEM is microverrucate: sculptural elements are of different sizes, mostly flattened, and scattered. Perforations are difficult to distinguish. In TEM the ectexine thickness varies from 0.38 to 1.0 μm in the regions of microverrucae or between them. Similarly, the tectum is from 0.1 to 0.52 μm thick. The canals through to the infratectum are occasionally seen. The columellae are from 0.08 to 0.13 μm high and from 0.08 to 0.44 μm wide. The foot layer is of an uneven thickness, though it is not often discontinuous and mostly between 0.04 and 0.15 μm. The probable endexine is slightly less electron dense, from 0.02 to 0.19 μm in thickness, with sharp drops of the thickness, forming pud-like regions.

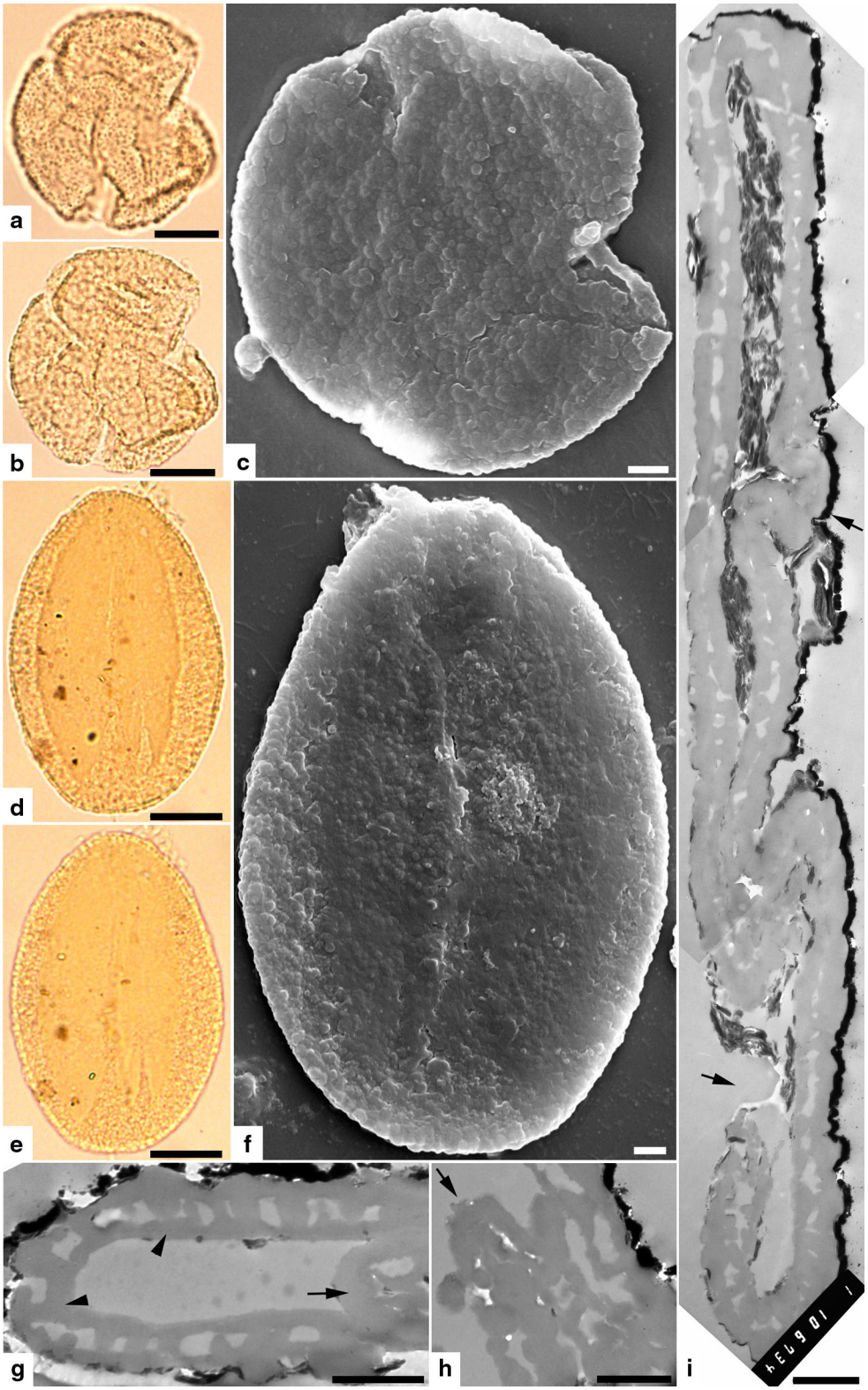

Fig. 8 Pollen morphology and ultrastructure of Group 7 (**a**–**i**). **a**, **b** LM, polar view, two different foci; **c** SEM, polar view; **d**, **e** LM, equatorial view, two different foci; **f** SEM, equatorial view; **g** TEM, nonaperture region; **h** TEM, aperture region; **i** TEM, section through the whole pollen. *Arrowheads* show border between ect- and endexine; *arrow* indicates aperture region. *Scale bar* is 1 μm for **g**–**i**; 2 μm for **f**; 3 μm for **c**; 10 μm for **a**, **b**, **d**, **e**

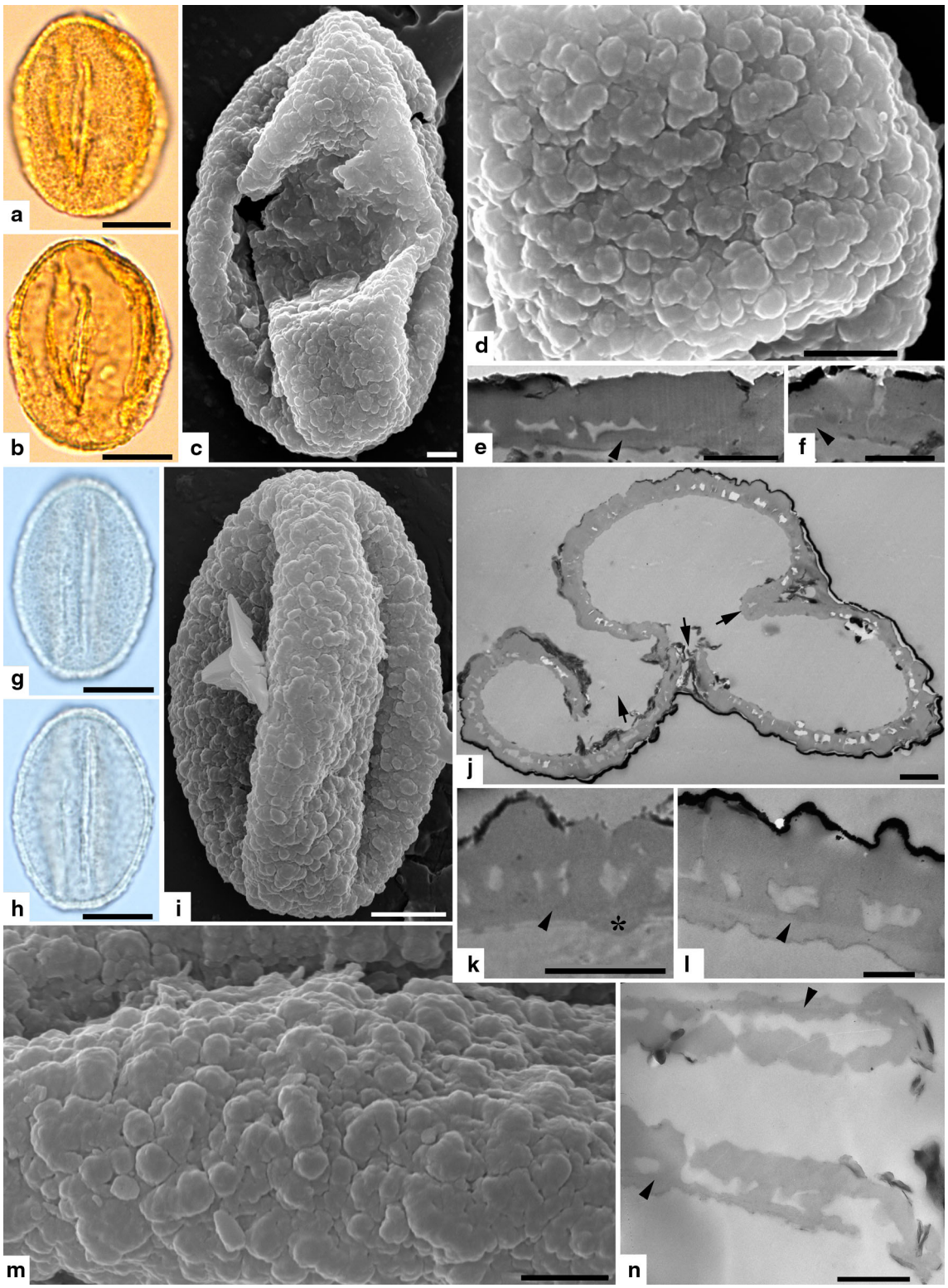

Fig. 9 Pollen morphology and ultrastructure of Group 8 (**a**–**f**) and Group 9 (**g**–**n**). **a**, **b** LM, equatorial view, two different foci; **c** SEM, equatorial view; **d** SEM, exine sculpturing; **e**, **f** TEM, nonaperture region; **g**, **h** LM, equatorial view, two different foci; **i** SEM, equatorial view; **j** TEM, section through the whole pollen; **k**, **l** TEM, nonaperture region; **m** SEM, exine sculpturing; n TEM, aperture region. *Arrowheads* show border between ect- and endexine; *asterisk* shows endexine drop; *arrow* indicates aperture region. *Scale bar* is 0.4 μm for **l**; 0.67 μm for **n**; 1 μm for **e**, **f**, **j**, **k**; 2 μm for **c**, **m**, **d**; 5 μm for **i**; 10 μm for **a**, **b**, **g**, **h**

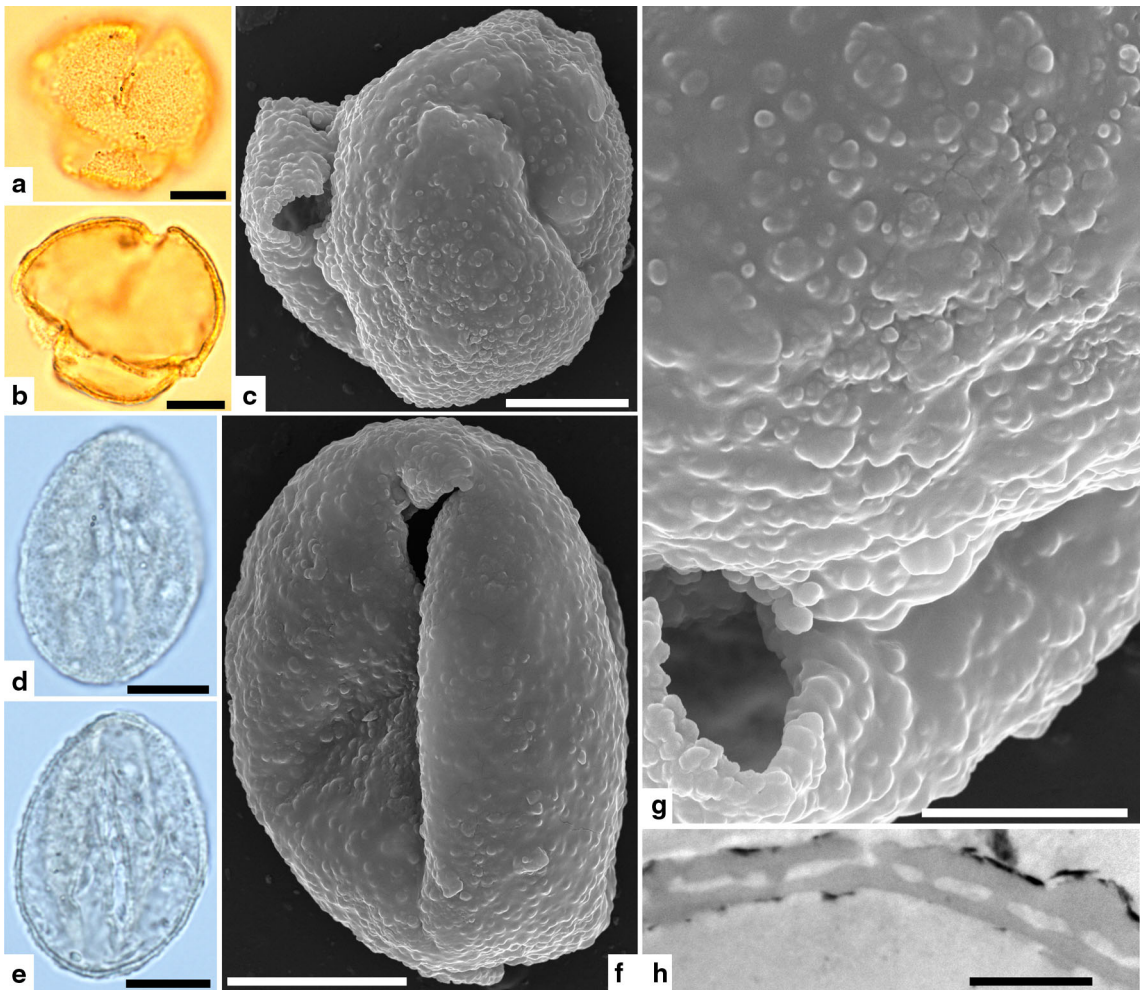

Fig. 10 Pollen morphology and ultrastructure of Group 10 (**a**–**h**). **a**, **b** LM, polar view, two different foci; **c** SEM, polar view; **d**, **e** LM, equatorial view, two different foci; **f** SEM, equatorial view; **g** SEM, exine sculpturing; **h** TEM, nonaperture region. *Scale bar* is 1 μm for **h**; 5 μm for **g**; 10 μm for **a**–**f**

Discussion

Based on the size and shape many researches distinguish pollen of evergreen and deciduous oaks or even detect them to the species level in LM, especially if in the studied region few oak species are expected to occur. While this is a quick and useful approach to estimate a general pattern of a pollen assemblage, there is always a risk of an erroneous interpretation or overlooked occasional pollen types. Also, this approach does not help much in case of the assemblage with mainly deciduous oaks. Pollen characters of modern *Quercus* species were explored by many researchers in the hope of finding any to distinguish between the species or groups of species, first with LM, then also with SEM and, rarely, with TEM. Thus, Monoszon (1954, 1961) studied in LM a number of oak species in search of diagnostic characters to distinguish *Quercus* to the specific level and with respect to the variability of their morphology (pollen size, exine thickness, sculpture). Mittre and Singh (1963) divided five species they studied into groups using polar axis and exine thickness. Yamazaki and Takeoka (1959), Dupont and Dupont (1972) discovered that the sculpture in SEM differed in the deciduous and evergreen oak species they studied. Smit (1973) established three pollen types using characteristics in SEM (exine sculpture, perforations, colpus membrane, and aperture) which include Yamazaki and Takeoka's and Dupont and Dupont's deciduous and evergreen groups and an intermediate (suber) group. He compiled the data so that the three types were: A. *Quercus robur/petraea* (*Q. robur*, *Q. petraea*, *Q. pubescens*, *Q. pyrenaica*, *Q. dentata*, *Q. pontica*, *Q. variabilis*, *Q. acutissima*, *Q. mongolica* var. *grosseserrata*, *Q. aliena, Q. serrata*, *Q. pedunculata* (=*Q. robur*), *Q. roza* and *Q. sessilifolia* (=*Q. petraea*)), B. *Quercus ilex/coccifera* (*Q. ilex*,

Q. coccifera, *Q. calliprinos*, *Q. phillyraeoides* and *Q. phillyraeoides* var. *crispa*) and C. *Quercus suber* (*Q. suber*, *Q. cerris*, *Q. macrolepis*, *Q. crenata*, *Q. trojana* and *Q. thraeiea*). Colombo et al. (1983) analyzed both SEM and TEM data of several oak species (the same that Smit (1973) had studied and classified). They supplemented Smit's data finding out that the edge of the aperture membrane (being rough or smooth), exine thickness in TEM (being the smallest in *Q. pubescens*), polar axis and equatorial diameter ranges, and presence/absence of the endoaperture differ in the three types or between *Quercus* species possibly allowing distinguishing them within the three groups. Also, they revealed a greater variability in the sculpture for C. *Quercus suber* type. Crepet and Daghlian (1980) distinguished two main sculpture types (verrucate and rod-like) among modern oak species they studied; they also performed a TEM study and revealed some, but not very clear differences between the distinguished types. Jarvis et al. (1992) distinguished pollen of deciduous and evergreen oaks among the studied material in LM with deciduous ones having coarser sculpture and rounder elements, with the margin of unchanging width along the apertures and lacking a distinct geniculus. Fujiki et al. (1996) studied some species of *Lepidobalanus*, deciduous oaks, and established two major types, striate (*Q. phillyraeoides*) and granulate with four subtypes (*Q. acutissima*, *Q. crispula*, *Q. aliena*, *Q. variabilis*, *Q. dentata*, and *Q. serrata*). Naryshkina (2013) studied pollen morphology of 24 *Quercus* species and made a detailed analysis of the characters (using morphological and statistical methods), revealing that the studied species can be divided into three groups concerning the pollen size, and into two groups by aperture condition; she established three general types and ten subtypes based on the exine sculpture in SEM. This allowed her to distinguish three large pollen types with subtypes within them.

In recent years, more and more works have been published on the pollen morphology and sometimes ultrastructure of modern *Quercus* species of different regions with respect to the systematics, ecology, hybridization, and phylogeny (e.g., Medus and Gonzalez-Flores 1984; Solomon 1983a, b; Shen and Liu 1984; Savitskii et al. 1999; Wang and Pu 2004; Denk and Grimm 2009; Makino et al. 2009; Panahi et al. 2012; Naryshkina 2013 and others).

On the whole, pollen characters such as size, shape, aperture condition, aperture membrane, exine sculpture, colpus margin, ectexine thickness, and presence/absence of perforations were found to be useful to distinguish *Quercus* pollen below the generic level. Researchers show different degrees of optimism in the possibility of distinguishing *Quercus* pollen to the species level, but it is evident that the taxon (or at least many of its species) possesses high morphological variability due to commonplace hybridization and interfertility among oak species. This complicates taxonomical attribution of dubious species/populations and requires knowledge (or studies) of the genetics of the considered populations and statistical studies of the pollen grains. Also it considerably ceases the reliability of the pollen determination, especially when we deal with small amounts of the material. Another difficulty concerns LM characteristics (such as exine sculpture and thickness) which, while more easily observed (and, thus, can be studied for more pollen grains), have lower resolution than in SEM or TEM (with elements looking different in SEM and being quite similar in LM, or exine thickness, which is evidently better to measure in TEM). Although not an original observation, or, honestly saying, quite a well known one, we still have this problem today and have to compare data studied in LM only, SEM only, or even in TEM only (Zheng et al. 1999)! With pollen size, measurements in LM and SEM differ (e.g., Denk and Tekleva 2006; Tschan et al. 2008; Naryshkina 2013, our data), so it is hard to compare pollen size groups of *Quercus* species studied by different methods. Another difficulty comes from comparing pollen characters observed in untreated, acetolyzed, and/or fossil material. Some of them might disappear completely or be significantly destroyed or altered (aperture characters, sculpture elements, colpus edge/margin, endexine and intine). Fossil oak material is represented at present mostly in a dispersed state uncovering therefore additional trouble of scarce quantity of pollen grains or even solitary pollen grains, and as in this case we cannot be 100 % sure that any two dispersed pollen grains belong to the same species. As a result, in case of fossil dispersed oak pollen, we should operate with some quite reliable qualitative characters, while quantitative ones can only give us some additional questionable support. Also, we should draw all information that we can obtain for the pollen grain, i.e., using LM, SEM, and TEM. But this is quite laborious. Another difficulty with oak pollen studied here is that the (micro)verrucate patterns seem to show more morphological variability than rod-like or rugulate–granulate patterns.

A number of studies are dedicated to fossil oaks species determination based on pollen grains, mostly in Japan, Korea, China, and Russia. LM and/or SEM methods were used to accomplish such a comparison with modern pollen morphology. Monoszon (1975) and Zernitskaya (1992) determined *Q. robur*, *Q. pubescens*, and *Q. petraea* with SEM. Nakagawa et al. (1996) distinguished *Q. semecarpifolia*, *Q. incana*, *Q. lanuginosa*, and *Q. glauca* with SEM. Fujiki with co-authors (Fujiki et al. 1996; Fujiki and Yasuda 2004) recognized oak species they had studied on modern material in the fossil assemblage (*Q. acutissima*, *Q. aliena*, *Q. crispula*, *Q. dentata*, *Q. serrata*, *Q. variabilis*). Ferguson et al. (1998) found two pollen types of oaks in the Miocene

deposits of Germany, but did not attribute them to any particular species. Kataoka (2006) described six pollen types corresponding to *Q. sessifolia*, *Q. glauca*, *Q. acutissima*, *Q. variabilis*, *Q. dentata*, and *Q. serrata*. Liu et al. (2007) made a comprehensive analysis of the known data on the oak pollen and established four general pollen types (sculpturing types) on the whole and nine morphotaxa in the deposits they studied. They did not correspond their morphotaxa with oak species, but indicated their possible deciduous or evergreen habit; so did Hofmann et al. (2002) and Van der Burgh and Zetter (1998) for the deposits of Austria and Germany, respectively. Hristova and Ivanov (2009) found pollen of *Quercus robur* type in the Miocene deposits of Bulgaria. Denk et al. (2010, 2012) described fossil oak pollen from Iceland and Central Europe with determination to infrageneric groups. Hayashi et al. (2012) identified four types of oak pollen grains: *Q. dentata* type (*Q. dentata*), *Q. phillyreoides* type (*Q. phillyreoides*), *Q.* sect. *Prinus* type (*Q. mongolica* var. *grosseserrata*, *Q. serrata*, *Q. aliena*), and *Q.* sect. *Cerris* type (*Q. variabilis*, *Q. acutissima*). The authors made conclusions on the ecology, paleogeography, and climatic changes of the studied regions. In general, the main character that most of the authors used to recognize fossil oak pollen was the exine sculpturing seen in SEM. Other characters (size, aperture condition) are rarely mentioned. The sporoderm ultrastructure has not been studied for fossil oak pollen so far.

Several works attempted to classify pollen grains of modern oaks based on the exine sculpture: Smit (1973) established three types (microverrucate, of elongated elements (=rod-like in terms of others), and an intermediate); Liu et al. (2007)—four types (scabrate–verrucate—Type 1, rugulate—Type 2, rod-like elements—Type 3, and finely granulate—Type 4); Makino et al. (2009)—two types (microspinulate and granulate) for *Quercus* subgenus *Cyclobalanopsis* and two types (striate and granulate with three subtypes) for *Quercus* subgenus *Lepidobalanus*; Denk, Grimm (2009)—five types (rod-like vertical, rod-like masked, rod-like (micro) rugulate, (micro) verrucate, and (micro) verrucate scattered); and Naryshkina (2013)—three types (verrucate, rugulate, and granulate) and ten subtypes. They mostly conform to each other, though disparity for some species/pollen types does exist.

The ten conventional groups in which we divided the studied dispersed pollen grains can be attributed to three general types of exine sculpturing: rod-like (Group 1), rugulate–granulate (Group 2) and (micro)verrucate (Groups 3–10). The sculpture type observed in Group 1 is characteristic for species from *Heterobalanus* and *Ilex* section (Type 3 sensu Liu et al. 2007); that of Group 2 in sections *Acuta, Gilva, Lobatae, Ilex, Quercus, Glauca, Cyclobalanoides, helferiana,* and *Protobalanus* (Type 2 sensu Liu et al. (2007); and that of Groups 3–10 in sections *Cerris*, *Quercus*, and, rarely *Ilex* (Type 1 sensu Liu et al. (2007). While the first two types can be easily separated (among studied pollen) groups 3–10 with the (micro)verrucate pollen are sometimes quite difficult to distinguish due to their overlaying variability and it is possible that some of these groups actually may belong to the one and the same. The commonplace hybridization and interfertility in oak species at least in a number of *Quercus* species likely influence the variability of the exine sculpturing that we see in some species (e.g., Makino et al. 2009). This makes it very difficult to distinguish these species with certainty on the dispersed material. Nevertheless, we can guess the possible attribution, especially studying Holocene material and comparing it with the modern *Quercus* species of the considered regions.

At present, these are *Q. acuta*, *Q. acutissima*, *Q. aliena*, *Q. dentata*, *Q. glauca*, *Q. mongolica* var. *grosseserrata* (=*Q. crispula*, according to Menitskij 1984; Shidei 1974; Takahara and Kitagawa 2000; Box and Fujiwara 2012), *Q. phillyraeoides*, *Q. serrata*, and *Q. variabilis* with three evergreen trees and shrubs (*Q. acuta*, *Q. glauca*, *Q. phillyraeoides*) and six deciduous trees with different ecological traits (Hayashi et al. 2012; Tsukada 1988). *Q. acutissima* and *Q. variabilis* belong to *Q.* sect. Cerris; *Q. aliena*, *Q. dentata*, *Q. mongolica*, *Q. serrata* belong to *Q.* sect. Quercus; *Q. phillyraeodies* belongs to *Q.* sect. Ilex; *Q. acuta* belongs to *Q.* sect. Acuta; *Q. glauca* belongs to *Q.* sect Glauca. Based on published data of the close regions (Hayashi et al. 2012; Makino et al. 2009; Fujiki et al. 1996; Fujiki and Yasuda 2004; Kataoka 2006; Naryshkina and Evstigneeva 2009; Evstigneeva and Naryshkina 2012; Naryshkina 2013), Group 1 nicely matches with *Q. semecarpifolia* type, Group 2 matches with *Q. gilva* type, Group 3 matches with *Q. aliena* type, Groups 4 and 5 match with *Q. dentata* type, Groups 6 and 9 match with *Q, mongolica* type, *Q. mongolica* subspecies, or *Q.* section *Prinus* type, Group 7 matches with *Q. variabilis* type, Group 8 matches with *Q. serrata* type, and Group 10 matches with *Q. crispula*. The terminology, used by Makino et al. (2009), Fujiki and Yasuda (2004), and Fujiki et al. (1996) and Hayashi et al. (2012) differs from that in the present paper. They use the term "granula" where we mostly use the term "verruca", and, thereby Makino et al. (2009) define round granula type for *Q. mongolica* var. *grosseserrata*, *Q. serrata*, and *Q. aliena*, sharp-pointed granula type for *Q. dentata*, and the cockled granula type for *Q. variabilis* and *Q. acutissima*. Fujiki et al. (1996) established four types for deciduous *Quercus* fossil pollen that they studied: **I.** coarse grain-type granula with not bulging granula subtype (*Q. crispula*), densely distributed granula subtype (*Q. acutissima*), and scattered granula subtype (*Q. aliena*); **II.** cereal-type granula for *Q. variabilis*; **III.** confetti-type granula for *Q. dentata*; **IV.** wart-granula type for *Q. serrata*. But on the

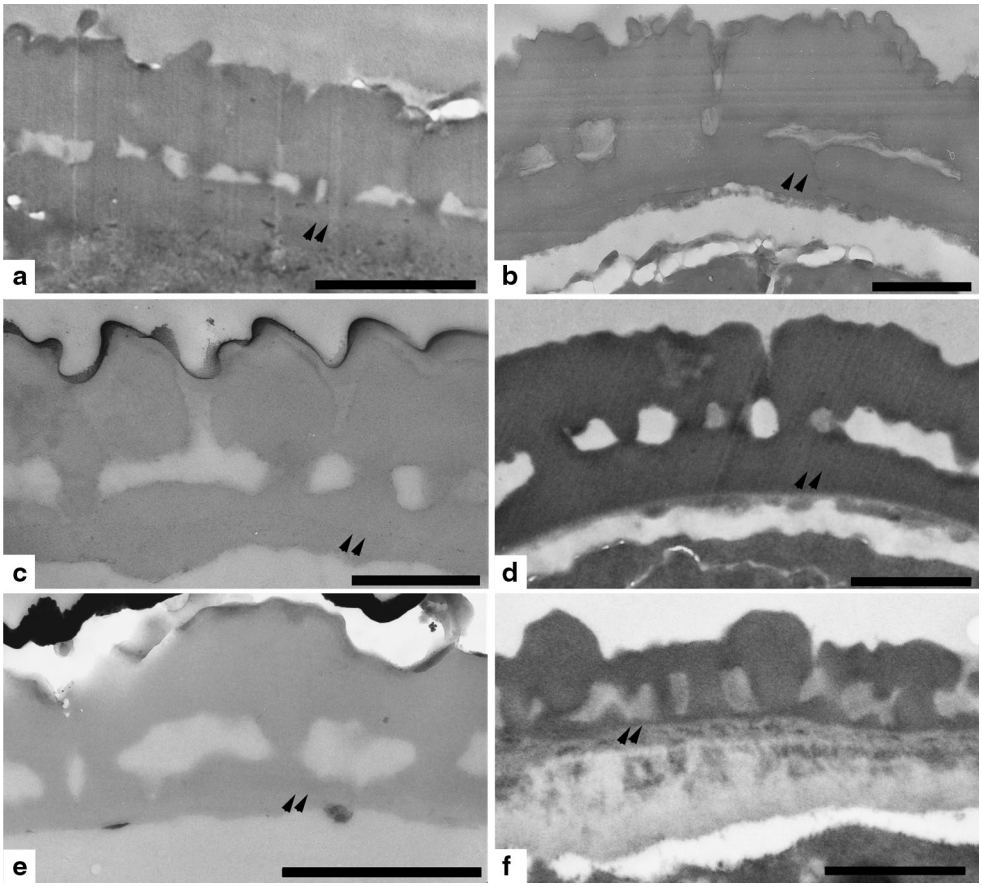

Fig. 11 Pollen ultrastructure in nonaperture regions for rod-like (**a**, **b**), rugulate-microechinate (**c**, **d**) and verrucate (**e**, **f**) types. a Group 1; **b** *Quercus semecarpifolia*; **c** Group 2; **d** *Quercus chrysolepis*; **e** Group 3; **f** *Quercus petraea*. *Arrowheads* show border between ect- and endexine. *Scale bar* is 0.5 μm for **c**; 0.67 μm for **b**; 1 μm for **a**, **d**–**f**

whole, the extracted types well corresponded with the scabrate–verrucate types, defined by other authors (e.g., Liu et al. 2007; Denk and Grimm 2009; Naryshkina 2013, etc.).

Pollen grains under study originate from two cores of the sediments of the Sea of Japan. Earlier, Naryshkina and Evstigneeva (2009) and Evstigneeva and Naryshkina (2012, 2013) recognized six types of fossil pollen from the same cores using SEM: four types, referring to deciduous oaks (*Q. mongolica* type or *Q. robur* type, *Q. variabilis* type, *Q. serrata* type, and *Q. dentata* type) and two of evergreen oaks (*Q. glauca* type and *Q. sessilifolia* type). Three of the types are verrucate and the other three are represented by verrucate–granulate, rugulate–echinate, and partially fused vertical rod-like elements. They compared the types with those known in the literature. Also they traced the quantitative distribution of the recognized types in the core depths and made important conclusions on the vegetation reconstruction of the studied regions. Our data mostly correspond with these earlier studies, though we have not found *Q. glauca* and *Q. sessilifolia* types, but probably *Q. aliena*, *Q. semecarpifolia,* and *Q. gilva* types. The absence of some pollen types in this study that were found before is not surprising. Few pollen grains of *Q. sessilifolia* were found in the Holocene optimum in the core 2747 from the shelf zone of the Korean Bay and were most probably transported by wind or water streams (Evstigneeva and Naryshkina 2012). Now the species grows in the south-east of China, Taiwan, and Japan (Honshu, Kyushu, Shikoku). *Q. glauca*, the pollen grains of which were also found in small amount in the studies by Evstigneeva and Naryshkina (2012, 2013) in the Holocene deposits of the Sea of Japan (core J3), today grows in the southernmost part of the Korean peninsula. The possible reason of its appearance in the spectrum can be due to the shift of evergreen forests to the north. Only solitary pollen grains (Groups 1 and 2) compared here with *Q. semecarpifolia* and *Q. gilva* types, respectively, were found during our study. The occurrence of random *Q. semecarpifolia* pollen can be explained by possible transporting by warm water streams of Kuroshio (Japan stream) from more southern regions (now it grows in Taiwan and China). On the other hand, *Quercus gilva* is a part of evergreen subtropical oak–laurel forests in Japan and it forms forests

also in the south of Honshu (Menitskij 1984); its small amount can be caused by different reasons.

On the whole studies of sporoderm ultrastructure give additional information on the exine patterns discriminated by means of LM and SEM and result in obtaining a complete image of a given pollen. Unfortunately, it still does not allow us to determine *Quercus* to the specific level in most cases, but gives more evidence for the established pollen types/groups. The suggested attribution of the revealed pollen groups to modern oak species corresponds well with published and original data on the sporoderm ultrastructure of modern oak pollen (Colombo et al. 1983; Crepet and Daghlian 1980; Kedves et al. 2002; Rowley and Gabaraeva 2004; Suárez-Cervera et al. 1994; Wang and Pu 2004; Zheng et al. 1999; Denk and Tekleva 2014; Fig. 11). On the average the tectum is thicker in Group 1 (Ilex section); the sharpest difference in the tectum thickness was observed in Group 5 (and probably Group 4). The infratectum thickness appears to be the smallest in Group 1. The foot layer, though discontinuous, probably on the average is thinner in Groups 3–10 in comparison to Groups 1 and 2. The canals through the tectum are common in Groups 1–3, rare in Groups 4–6, and occasionally occur in 7–10. In spite of the conclusion about the lower resistance of the ectexine in *Quercus* species (by Kedves et al. 2002), pollen of this type is abundant in Tertiary and Quaternary deposits, and we did not find any traces of ectexine damage in our material. Another interesting observation considering the fine structure of oak pollen was made by Rowley and his co-authors in a number of studies where they used oxidation treatment (acetolysis followed by potassium permanganate) and examined corroded exines from Havinga's leaf mold experiment (Rowley and Skvarla 1994; Rowley and Gabaraeva 2004; Skvarla et al. 1996). They showed on *Quercus robur* that there were two different sculpture patterns before and after the oxidation treatment—(micro)verrucate (in untreated *Q. robur*) and rod-like (in the oxidated one). They hypothesized that the rod-like pattern revealed after oxidation treatment is represented by tuft units and it is masked later by the secondarily deposited sporopollenin appearing as (micro)verrucate pattern. Furthermore, Denk and Grimm (2009) suggested that rod-like pattern ("*Ilex* pattern", tufts) corresponds to early developmental stages observed in infrageneric groups such as *Quercus* and *Lobatae*, and that later in the development these tufts can be masked by the secondarily deposited sporopollenin to a various extent (as in mature pollen of *Protobalanus* or *Cerris* infrageneric groups) and up to (micro)verrucate pattern in *Quercus* and *Lobatae* infrageneric groups. One of the still pending loose ends in the theory is that the tectum thickness in *Quercus* species with rod-like pattern is in most cases smaller than that of (micro)verrucate *Quercus* pollen, and pollen sections of rugulate–granulate oaks are also shown for comparison (Fig. 11a–f). Unfortunately, Rowley and Gabaraeva (2004) have made the oxidation experiment with *Quercus robur* only on the SEM level. So the TEM study of such pollen is necessary to check the theory and the work is in progress (Polevova and Tekleva, unpublished).

Acknowledgments The work was performed at User Facilities Center of M.V.Lomonosov Moscow State University under the financial support of the Ministry of Education and Science of the Russian Federation and at User Facilities Center of A.A. Borissiak Paleontological Institute, Russian Academy of Sciences. The study was supported by the Russian Foundation for Basic Research grant # 12-04-01740-a, by the grant by President RF MK-3156.2014.4 and by the Presidium of the Russian Academy of Sciences, # 14-III-B-06-041.

References

Box EO, Fujiwara K (2012) A comparative look at bioclimatic zonation, vegetation types, tree taxa and species richness in northeast Asia. Botanica Pacifica 1:5–20

Colombo PM, Lorezone FC, Grigoletto F (1983) Pollen grain morphology supports the taxonomical discrimination of mediterranean oaks (*Quercus*, Fagaceae). Plant Syst Evol 141:273–284

Crepet WL, Daghlian CP (1980) Castaneoid inflorescences from the Middle Eocene of Tennessee and the diagnostic value of pollen (at the subfamily level) in the Fagaceae. Am J Bot 67(5):739–757

Denk T, Grimm GW (2009) Significance of pollen characteristics for infrageneric classification and phylogeny in *Quercus* (Fagaceae). Int J Plant Sci 170:926–940

Denk T, Tekleva MV (2006) Comparative pollen morphology and ultrastructure of *Platanus*: implications for phylogeny and evaluation of the fossil record. Grana 45:195–221

Denk T, Tekleva MV (2014) Pollen morphology and ultrastructure of *Quercus* with focus on Group Ilex (=*Quercus* Subgenus *Heterobalanus* (Oerst.) Menitsky): implications for oak systematics and evolution. Grana (in press)

Denk T, Grimsson F, Zetter R (2010) Episodic migration of oaks to Iceland: evidence for a North Atlantic "land bridge" in the latest Miocene. Am J Bot 97(2):276–287

Denk T, Grimsson F, Zetter R (2012) Fagaceae from the early Oligocene of Central Europe: persisting new world and biogeographic links. Rev Palaeobot Palynol 169:7–20

Dupont R, Dupont S (1972) Etude de pollens de chênes (genre *Quercus* L.) en microscopie électronique à balayage. C R Séances Acad Sci Ser D 274(17):2503–2506

Evstigneeva TA, Naryshkina NN (2012) Holocene vegetation changes on the north-eastern coast of the Korean Peninsula based on the palynological data. Acta Palaeobot 52(1):147–155

Ferguson DK, Pingen M, Zetter R, Hofmann C–C (1998) Advances in our knowledge of the Miocene plant assemblage from Kreuzau, Germany. Rev Palaeobot Palynol 101:147–177

Fujiki T, Yasuda Y (2004) Vegetation history during the Holocene from Lake Hyangho, northeastern Korea. Quart Int 123(125):63–69

Fujiki T, Morita Y, Miyochi N (1996) Pollen morphology of subgenus *Lepidobalanus* (*Quercus*, Fagaceae) in Japan. Jpn J Palynol 42:107–116

Hayashi R, Inoue J, Makito M, Takahara H (2012) Vegetation history during the last 17000 years around Sonenuma Swamp in the eastern shore area of lake Biwa, western Japan: with special reference to changes in species composition of *Quercus* subgenus *Lepidobalanus* trees based on SEM pollen morphology. Quart Int 254:99–106

Hesse M, Halbritter H, Zetter R, Weber M, Buchner R, Frosch-Radivo A, Ulrich S (2009) Pollen terminology—an illustrated handbook. Springer, New York

Hofmann C–C, Zetter R, Draxler I (2002) Pollen- und Sporenvergesellschaftungen aus dem Karpatium des Korneuburger Beckens (Niederösterreich). Beiträge zur Paläontologie Österreichs 27:17–43

Hristova V, Ivanov D (2009) Scanning electron microscope and light microscope study of selected palynomorphs from late Miocene sediments of Sofia Basin, Southwest Bulgaria. Geologica Balcanica 38(1–3):53–58

Jarvis DI, Leopold EB, Liu Y (1992) Distinguishing the pollen of deciduous oaks, evergreen oaks, and certain rosaceous species of southwestern Sichuan Province, China. Rev Palaeobot Palynol 75:259–271

Kataoka H (2006) Pollen analytical study of sediments from Koigakubo moor, Okayama. Naturalistae 10:47–54

Kedves M, Párdutz Á, Varga B (2002) Experimental investigations on the pollen grains of *Quercus robur* L. Taiwania 47(1):43–53

Liu YS, Zetter R, Ferguson DK, Mohr BAR (2007) Discriminating fossil evergreen and deciduous *Quercus* pollen: a case study from the Miocene of eastern China. Rev Palaeobot Palynol 145:289–303

Makino M, Hayashi R, Takahara H (2009) Pollen morphology of the genus *Quercus* by scanning electron microscope. Life Environ Sci 61:53–81

Medus J, Gonzalez-Flores G (1984) Pollen morphology of some Mexican oaks. Grana 23(2):77–84

Menitskij YL (1984) Oaks of Asia. Nauka, Leningrad (in Russian)

Meyer-Melikyan NR, Bovina IY, Kosenko YV, Polevova SV, Severova EE, Tekleva MV, Tokarev PI (2004) Atlas of morphology of Asterales (Asteraceae). Palynomorphology and the development of sporoderm in members of the family Asteraceae. KMK, Moscow

Mittre V, Singh G (1963) On the pollen of the western Himalayan oaks. J Ind Bot Soc 42(1):132–134

Monoszon MH (1954) A morphological description of main oak species on the USSR territory. Proc Inst Geogr USSR 61:93–118 (in Russian)

Monoszon MH (1961) On the variation of morphological characters of some oaks. Rep USSR 140(6):1456–1459 (in Russian)

Monoszon MH (1975) An attempt of SEM study of fossil pollen for diagnostics. Bull USSR Ser Geogr 6:110–116 (in Russian)

Nakagawa T, Yasuda Y, Tabata H (1996) Pollen morphology of Himalayan *Pinus* and *Quercus* and its importance in palynological studies in Himalayan area. Rev Palaeobot Palynol 91:317–329

Naryshkina NN (2013) Morphology of recent and fossil pollen of some *Quercus* L. species. Dissertation, Institute of Biology and Soil Science of Far Eastern Branch of Russian Academy of Sciences

Naryshkina NN, Evstigneeva TA (2009) Sculpture of pollen grains of *Quercus* L. from the Holocene of the south of the sea of Japan. Paleontol J 43(10):1309–1315

Panahi P, Pourmajidian MR, Fallah A, Pourhashemi M (2012) Pollen morphology of *Quercus* (subgenus *Quercus*, section *Quercus*) in Iran and its systematic implication. Acta Societatis Botanicorum Poloniae 81(1):33–41

Rowley JR, Gabaraeva NI (2004) Microspore development in *Quercus robur* (Fagaceae). Rev Palaeobot Palynol 132:115–132

Rowley JR, Skvarla JJ (1994) Corroded exines from Havinga's leaf mold experiment—structure of *Fagus* and *Quercus* exines. Rev Palaeobot Palynol 83:65–72

Savitskii VD, Martynuk OO, Shumik MI (1999) Palynomorphological features of *Quercus* species in Ukraine. Ukr Bot J 56(1):33–35 (in Russian)

Shen C-F, Liu T-S (1984) The taxonomy and pollen morphology of the Fagaceae in Taiwan. Epoch Publishing Co. Ltd, Taipei

Shidei T (1974) Forest vegetation zones. In: Numata M (ed) The flora and vegetation of Japan. Kodansha Ltd./Elsevier Scientific Publ. Co., Tokyo/Amsterdam, pp 87–124

Skvarla JJ, Rowley JR, Chissoe WF (1996) Corroded exines from Havinga's leaf mold experiment. SEM. Palynology 20:191–207

Smit AA (1973) A scanning electron microscopical study of the pollen morphology in the genus *Quercus*. Acta Bot Neerl 22:655–665

Solomon AM (1983a) Pollen morphology and plant taxonomy of white oaks in eastern North America. Am J Bot 70:481–494

Solomon AM (1983b) Pollen morphology and plant taxonomy of red oaks in eastern North America. Am J Bot 70:495–507

Suárez-Cervera M, Marquez J, Bosch J, Seoane-Camba J (1994) An ultrastructural study of pollen grains consumed by larvae of *Osmia* bees (Hymenoptera, Megachilidae). Grana 33(4):191–204

Takahara H, Kitagawa H (2000) Vegetation and climate history since the last interglacial in Kurota Lowland, western Japan. Palaeogeogr Palaeoclimatol Palaeoecol 155(1):123–134

Tschan GF, Denk T, Von Balthazar M (2008) *Credneria* and *Platanus* (Platanaceae) from the Late Cretaceous (Santonian) of Quedlinburg, Germany. Rev Palaeobot Palynol 152:211–236

Tsukada M (1988) Japan. Vegetation history. Kluwer, Dorbrecht

Van Benthem F, Clarke G, Punt W (1984) Fagaceae. In: Punt W, Clarke GCS (eds) The Northwest European Pollen Flora, vol 4, no. 33, pp 87–110

Van der Burgh J, Zetter R (1998) Plant mega- and microfossil assemblages from the Brunssumian of "Hambach" near Düren, B.R.D. Rev Palaeobot Palynol 101:209–256

Wang P, Pu F (2004) Pollen morphology and biogeography of Fagaceae. Guangdong Science and Technology Press, Guangzhou (in Chinese)

Yamazaki T, Takeoka M (1959) Electron microscope investigations on the surface structure of the pollen membrane, based on the replica method. B. Especially on the pollen genus *Quercus*. J Jpn Forest Soc 41:125–130

Zernitskaya VP (1992) Pollen of *Quercus* (Fagaceae) from late glacial and Holocene deposits of Belarus. Bot J 77(11):71–74 (in Russian)

Zheng ZH, Wang PL, Pu FD (1999) A comparative study on pollen exine ultrastructure of *Nothofagus* and the other genera of Fagaceae. Acta Phytotaxonomica Sinica 37(3):253–258